Geocarto International
Publication details, including instructions for authors and subscription information:
http://www.tandfonline.com/loi/tgei20

Semi-automatic delineation of badlands using contrast in vegetation activity: A case study in the lower Chambal valley, India

V. Ranga[ab], A. Van Rompaey[a], J. Poesen[a], S.N. Mohapatra[b] & P. Pani[c]

[a] Division of Geography, Department of Earth and Environmental Science, K.U. Leuven, Belgium

[b] Centre of Remote Sensing & GIS, School of Studies in Earth Sciences, Jiwaji University, Gwalior, India

[c] Centre for the Study of Regional Development, Jawaharlal Nehru University, New Delhi, India

Accepted author version posted online: 07 Jan 2015.

To cite this article: V. Ranga, A. Van Rompaey, J. Poesen, S.N. Mohapatra & P. Pani (2015): Semi-automatic delineation of badlands using contrast in vegetation activity: A case study in the lower Chambal valley, India, Geocarto International, DOI: 10.1080/10106049.2015.1004130

To link to this article: http://dx.doi.org/10.1080/10106049.2015.1004130

Publisher: Taylor & Francis
Journal: *Geocarto International*
DOI: http://dx.doi.org/10.1080/10106049.2015.1004130

Semi-automatic delineation of badlands using contrast in vegetation activity: A case study in the lower Chambal valley, India.

V.Ranga[a,b*], A. Van Rompaey[a], J.Poesen[a], S.N. Mohapatra[b] and P. Pani[c]

[a] Division of Geography, Department of Earth and Environmental Science, K.U. Leuven, Belgium.

[b] Centre of Remote Sensing & GIS, School of Studies in Earth Sciences, Jiwaji University, Gwalior, India.

[c] Centre for the Study of Regional Development, Jawaharlal Nehru University, New Delhi, India.

Abstract

Population growth worldwide leads to an increasing pressure on the land. Recent studies reported that many areas covered by badlands are decreasing because parts of badlands are being levelled and converted into arable land. It is important to monitor these changes for environmental planning. This paper proposes a remote-sensing based detection method which allows mapping of badland dynamics based on seasonal vegetation changes in the lower Chambal valley, India. Supervised classification was applied on three Landsat (*Thematic Mapper*) images, from 3 different seasons; January (winter), April (summer) and October (post-monsoon). Different band selection methods were applied to get the best classification. Validation was done by ground referencing and a GeoEye-1 satellite image. The image from January performed best with overall accuracy of 87% and 0.69 of kappa. This method opens the possibilities of using semi-automatic classification for the Chambal badlands which is so far mapped with manual interpretations only.

Key-words: NDVI time series analysis, badlands, image classification, lower Chambal Valley.

1. Introduction

The present scenario of increase in population worldwide requires increase in food production (Byrnes & Bumb 1998; Gilland 2002), which has, in turn, created pressure on available land and caused humans to encroach on highly degraded land such as badlands. Many studies in the past decade (Poesen & Hooke 1997; Phillips 1998; Borselli et al. 2006) have illustrated the processes of encroachment on badlands by land levelling (by bulldozing, sedimentation etc.) and since they reduce soil quality, levelling of badlands should be considered a soil degradation process (Poesen & Hooke 1997). Badlands constitute dynamic environments where they are formed, expand and disappear or are deleted following the changes in the equilibrium between natural processes and human activities (Torri et al. 2000). In arid and semi-arid regions where vegetation is very sparse and soils are rich in clay minerals, severe erosion induces the badlands, characterized by steep slopes with rills and gullies as their main features (Liberti et al. 2009). In India,

although badlands are found along most of the rivers (Chatterjee et al. 2009), they are most prominent in four scattered parts i.e. the Yamuna-Chambal region, the sub-Himalyan zone in Punjab, the Gujarat plains and the Chota Nagpur plateau (Sharma 1979). Out of these, badlands found along the Chambal and its tributaries are the most severely incised and degraded (Sharma 1979). The badlands of the Chambal valley are subjected to levelling processes but the levelling is not sustainable and requires continuous efforts (Ranga 2013). Being an agriculture dependent economy, India suffers great economic loss to badlands. Therefore, monitoring of badlands becomes an important aspect for policy making and environmental planning.

Remote sensing is an efficient complement to field methods to map gully development at specific time intervals; gullies are often developed in ramified badlands which are easier to map (Zinck et al. 2001). Field observations are generally restricted to short time periods (Sharma, 1979; Oostwoud Wijdenes et al., 2000; Vandekerckhove et al., 2001). However, if combined with aerial photography, they can be used for medium to long term studies (Seginer 1966; Sneddon et al., 1988; Nachtergaele and Poesen 1999; Ciccacci et al., 2009; Marzolff et al., 2011). Since satellite images do not provide the required high spatial resolution until recently, they can only be used for recent source of information but can be combined with archive aerial photograph for higher temporal resolutions. The use of satellite images to study badlands varies from the classification of badlands through manual interpretation (Singh 1977; Singh 1984; Sujatha et al. 2000; Dwivedi & Ramana 2003; National Remote Sensing Centre, India 2011) to more sophisticated spectral analysis (Zinck et al., 2001; Beguería, 2006; Alatorre and Beguería, 2009; Liberti et al., 2009; Nadal-Romero et al., 2012). Various researchers used a variety of approaches such as Zinck et al. (2001), who incorporated Landsat with JERS-1 SAR (L-band); Beguería (2006) used multinomial logistic regression to classify badlands in the Spanish Pyrenees; Liberti et al. (2009) mapped badlands effectively by combining spectral information with slope and aspect from a digital elevation model (DEM); Alatorre and Beguería (2009) used the receiver operating curve to define the threshold for badland areas while Nadal-Romero et al. (2012) used NDVI to assess the dynamics of badlands. Ideally, different combinations of these techniques should be applied to map badlands effectively because accurate detection of gullies and badlands requires

knowledge about the relationship between gullies development and their characteristic features to improve the between-class spectral separability (Zinck et al. 2001). Up to now, only manual interpretation of remote sensing image was applied in the lower Chambal valley badlands (Singh 1977; Singh 1984; Sujatha et al. 2000; Pani & Mohapatra 2001; Dwivedi & Ramana 2003; National Remote Sensing Centre, India 2011), and no attempt has been made of using spectral classification of satellite images for this area.

The complex spectral behaviour of natural soil is still a hindrance to multi-spectral satellite classification and different topsoil characteristics cause problems in discriminating the spectral signature of different eroded materials when using limited spectral bands (Liberti et al. 2009). However if vegetation can be used to differentiate various land use/cover classes; vegetation can, actually, form a basis for their spectral classification. In the lower Chambal valley, Singh (1977) observed that the tonal variation in Landsat images between badlands and croplands is mainly due to moisture retention by the soil and vegetation cover. Dwivedi and Raman (2003) noticed tonal differences in post-monsoon vegetation response in the badlands which appeared as different shades of red in False Colour Composite (FCC; combination: red:NIR; blue:Visual Spectrum (VIS)-Red; green:VIS-blue) of LISS-III image, while in pre-monsoon season it appears bluish green to greenish blue, indicating senesced or dry vegetation.

This paper 1) reports seasonal vegetation variations in different land use/cover classes and 2) identifies the most suitable season and band combination which should be used for a semi-automatic classification of badlands.

2. Study Area

The study area is located in Morena tehsil (sub-district) of the Morena distrtict of the Madhya Pradesh state in India. The study area covers ca. 100 km^2 between 26º 33′ to 26º 43′N latitude and 77º 55′ to 78º 05′E longitude. The badlands are, characteristically, formed in this region on both side of the Chambal River and its tributaries. The area belong to the marginal Gangetic Plains and is covered with thick alluvium with distinct fluvial landforms i.e. badlands (Figure 1). Incision of badlands can reach up to a

maximum depth of ~30m. Habib (1963) designated badlands in India as a pre-Mughal phenomenon (i.e. before 1526 AD) though no historical records were found to trace their formation (Singh & Agnihotri 1987). Badlands along the lower Chambal valley are getting levelled manually and the use of tractors and bulldozers leave them with a rolling topography rather than a flat one. Completely or near completely levelled land is normally found either in the badland valley bottoms or in remnants of dried channel meanders. The more undulating levelled land seems to be the work of tractors or bulldozers with clear signs of scouring (Ranga 2013).

The climate of the study area has three main seasons i.e. a summer, rainy and winter. The summer season extends from March to June, the rainy season from July to September and the winter season from October to February. The climate of the study area can be classified as warm temperate (**C**) steppe (**S**) with hot summers (**a**) i.e. **Csa** according to the updated Köppen-Geiger classification (Kottek et al. 2006). The average annual rainfall of Morena tehsil (subdistrict) is 796 mm (calculated from data acquired from Indian Metereological Data, Pune). As the annual rainfall exceeds 700 mm, badlands, in this area, can be classified as humid (see details in: Gallart et al 2013). The location map of the study area is shown in Figure 2.

3. **Datasets & Methodology**

This section describes the datasets and methodology used in analyzing seasonal vegetation variation, spectral separability of land use/cover (LULC) classes from satellite images, classification and accuracy assessment. Datasets and related methodology are not separately explained rather both are addressed together under the relevant subsections.

3.1 Satellite Images for LULC classification

In this study very high and moderate resolution satellite images have been used. Very high resolution images included an image from CORONA mission (acquisition = September' 1971, spatial resolution = 1.8 m at nadir) (see details in: McDonald (1995); Sohn et al (2004)) and a GeoEye Image from GeoEye-1 satellite (acquisition = June' 2010, spatial resolution = 0.5 m for panchromatic) (Geo Eye 2009). Since the GeoEye image shipped geo-rectified it could be used along with moderate resolution satellite

image for on-computer interpretation. Subsequently, the GeoEye image was taken in a laptop to field and interpretations of LULC were verified using a hand-held Garmin e-trex vista GPS device. Moderate resolution satellite images included three images from Thematic Mapper (TM) (spatial resolution = 30 m) onboard Landsat 5. Thermal bands were not used; only visible, NIR (*Near Infra-red)* and SWIR (*Short wave Infra-red)* were used. Three TM images were selected to study differences in spectral signatures due to different seasonal vegetation patterns; the images are from winter (16 January 2011), pre-monsoon (03 April 2010) and post-monsoon (28 October 2010). The dates of the image acquisitions were selected on the basis of availability and percentage of cloud cover. To insure spectrally unbiased classification, the top-of-atmosphere rectification method was used for atmospheric corrections; digital numbers were calibrated and converted to top-of-atmosphere reflectance (Chander et al. 2009) with Landsat package (Goslee 2011) in statistical software R (R Development Core Team 2011). Landsat images were used for supervised classification.

The dynamics of badlands was studied using four LULC classes i.e. water bodies, badlands, croplands and levelled land. The badlands are defined as densely dissected areas by mainly fluvial erosion with rills and gullies as their main features. Thus, the badlands class is given to land which is highly dissected (Figure 3a and 4a) with no signs of agriculture practices or scouring by tractors or bulldozers. Cropland, on the other hand, is nearly flat land with rectangular discernible agricultural plots and these plots are without any noticeable dissection due to fluvial erosion (Figure 3a and 4a). Levelled land is a transitory class between badlands and cropland. Identification of levelled land was achieved using CORONA and GeoEye images. Levelled land was defined as areas which were under badlands in the year 1971, as interpreted from the CORONA image, but found levelled in 2010, as interpreted from the GeoEye image. Levelled land (Figure 3b-c and 4b-c) is highly vulnerable to erosion and due to its convex topographic nature it is difficult to cultivate and manage. Other satellite products such as NDVI (Normalised Difference Vegetation Index) were also used to study vegetation activity in different LULC and are described in the section below.

3.2 MODIS NDVI time series analysis

Images from the MODIS (*Moderate Resolution Imaging Spectroradiometer*) sensor which is on board the Earth Observing System Terra as well as the Aqua satellites (http://modis.gsfc.nasa.gov/about/) was used in this study for NDVI values (and hence vegetation activity). Vegetation indices from MODIS are designed to provide consistent, spatial and temporal information of global vegetation conditions (Huete et al. 2002). MODIS provides a range of products with different spatial resolutions; this study used MYD13Q1 (onboard Aqua) due to its better spatial resolution i.e. 250 m than other MODIS products. Additionally, it always provides a well-timed NDVI value for each pixel even in persistent cloud cover or bad quality during 16-day period (Vrieling et al. 2008). NDVI is a vegetation index which ranges from -1 to +1 where, negative values are generated from water; around zero values generated from non-vegetated surfaces i.e. bare rocks, bare soil etc. (Silleos et al. 2006) while the increasing values towards positive one represent healthy vegetation activity. NDVI is one of the most used vegetation indices because it is successful as a vegetation measure and is sufficiently stable to allow meaningful comparisons of seasonal and inter-annual changes in vegetation growth and activity (Huete et al. 2002). LULC classes were identified on the GeoEye image & CORONA image as described in section above and 38 points on each land use class were allocated on pure pixels (pixels representing only one LULC class). Mean values of these 38 points for each month were used for plotting graphs and analysis.

An NDVI time series of 12 years (2001-2012) for the month of January was used to assess the evolution of vegetation activity on the levelled land. A rank based correlation coefficient between NDVI values and years was computed to investigate whether vegetation activity has increased over the last 12 years. Spearman's Rho suits the requirement well; therefore the correlation coefficient was calculated using R (R Development Core Team 2011).

3.3 Spectral Classification

A supervised classification (see: Lillesand & Kiefer (1987)) was performed, classifying four LULC classes i.e. 1) water bodies, 2) badlands, 3) cropland and 4) levelled land. The training pixels were selected with help of GeoEye satellite image. The same pixels were used for training the classification algorithm as well as to make spectral response

curves. The maximum Likelihood Classifier was used to classify the images. Since highest feature separability does not necessarily result from the maximum number of bands (Metternicht & Zinck 1998; Vrieling et al. 2007), three band selection methods i.e. *Correlation-Variance* (CV), *Transformed Divergence* (TD) distance and *Jaffries-Matusita* (JM) distance (Vrieling et al. 2007) were used. Initially, classification accuracy was assessed by using three different images from different seasons of a year; then the image with the highest classification accuracy was used to assess the best band combination by three aforementioned different methods (CV, TD and JM). In the CV method, correlation between all different pairs of bands and variance of each individual band were calculated; for the two highest correlating bands, the one with the lower variance was removed (Vrieling et al. 2007). TD and JM calculate distances between the two signatures from different classes. A band with least distance among the signature classes was removed at each step. This step was repeated until the desired number of bands remained; least number of bands was restricted to 3. The other two distance methods give the distance between the two classes; greater the distance, better the separability. The optimal number of bands was determined from the best combination with the highest separability. Composites of selected bands were then classified with the maximum likelihood classifier and their accuracy assessed as described in section below. To reduce the noise in the classification, 3×3 majority filter was used.

3.4 Accuracy assessment

Ground truth surveys were carried out in the month of June during the year 2011. Accuracy of TM images was accessed using GeoEye satellite image. As it was shown by Plourde & Congalton (2003) that systematic sampling does not affect the variance of accuracy significantly, so the systematic sampling design, with 1177 equally spaced sample points at every 300 m was used. Classification accuracy of the whole area was assessed by estimating Producer's accuracy (PA), User's Accuracy (UA), Overall Accuracy (OA) and Kappa statistics (K) calculated from the error matrix

To do so, an error matrix was created by making a cross-tabulation where columns represented reference data while rows represented classified data of LULC classes. Diagonal values are truly classified pixels and they are used to calculate *overall accuracy*

i.e. ratio of cumulative diagonal values to the total pixels in the error matrix; while the non-diagonal values represented errors. If the errors are estimated through columns i.e. proportion of diagonal value divided by total cumulative value of a given column, it gives *producer's accuracy* or *error due to omission*. On the other hand, if errors are estimated through row it is termed as *user's accuracy* or *error due to commission*. As the name suggests, error due to commission occurred when pixels of a category wrongly assigned to another category by classification, thus adding erroneous pixels to a LULC class. On the contrary, producer's accuracy can be opposite of addition i.e. omission. Additionally, kappa incorporates these errors with overall accuracy and gives a figure which can be interpreted as percent to that classification is better than the random coincidence of the two datasets. Since it is hard to specify one single measure to assess the overall accuracy of the classification (Foody 2002), all the aforementioned parameters were considered to evaluate the best possible accuracy.

4 Results and Discussion

4.1 NDVI time series analysis

Following the chronology of research objectives, this section explains seasonal variations of vegetation. Out of three LULC classes, NDVI values of cropland and levelled land closely follow each other and have same trend (Figure 5). Both the classes exhibit two distinct peaks representing two cropping seasons i.e. 1) *Kharif* (wet) season and 2) *Rabi* (dry) season. The kharif season starts with the onset of monsoon and sowing usually completed by the middle of July. First peak (Figure 5) which starts from July corresponds to this season. Main crops of this season are pearl millet (*pennisetum glaucum*), lentils (such as: *cajanus cajan*), sesame (s*esamum indicum*), etc. Rabi season starts from the month of October and this corresponds to the starting of second peak in figure 5. Rabi season ends with the harvesting in the month of March-April. Main crops of rabi season are wheat (*triticum aestivum*), mustard (*brassica juncea*) etc. The only difference between NDVI values of cropland and levelled land is that the values of the latter are smaller than the former. These two classes have similar trend; this can be attributed to similar land use in both of them i.e. cultivation. On the other hand, the difference, in

mean values of NDVI, between these classes can be attributed to sparse cropping due to rolling topography (Figure 4c) and hence lower NDVI values of levelled land.

Vegetation activity (NDVI values) in badlands, on the contrary, shows only one peak starting on the onset of monsoon. This increased growth of vegetation starts fading away with the fading monsoon and vegetation in badlands eventually reduced to minimum during summers. The maximum difference, in terms of NDVI values, between badlands and other two classes is in the months of January-February and September-October. Three different seasons i.e. the month of January (winters), April (summer/pre-monsoon) and, October (post-monsoon) were chosen to further investigate the suitability of vegetation as mapping aid and tool. The January was chosen for showing highest vegetation contrast between badlands and croplands, April was chosen for showing least vegetation cover in both the aforementioned classes while October was chosen because vegetation activity in LULC classes is just opposite as that in January. Figure 6 confirms the distinction between badlands and other two classes in terms of vegetation. The month of April (Figure 6b) shows vegetation patches all over the image and does not represent a clear distinction as in other two seasons (Figure 6a & 6c). These vegetation patches (Figure 6b) are irrigated cultivation and due to scarcity of water in summers, limited only to certain patches.

Results of this analysis are quite different to what has been reported from badlands in other parts of the world, especially, in Spain. Alatorre et al (2011) and Nadal-Romero et al (2012) have reported a negative trend in vegetation activity in badlands in the Central Spanish Pyrenees thus highlighting progressive soil degradation. Furthermore, there is no sharp inter-season contrast in vegetation activity reported, as demonstrated in this study. Regional vegetation knowledge, therefore, can be very useful in affective regional planning. E.g. after aerial seeding of Chambal valley to control soil erosion; Adams (1987), on finding the effort ineffective, suggested grass buffer strips for the same purpose. As noticed in this study, the grass or other vegetation variety for this purpose should be summer tolerant to be affective.

Vegetation activity in badlands is also indicative of erosion processes. Vegetation has a stabilizing affect to soil erosion; in Chambal valley increase in vegetation after the

monsoon may be indicative of reduction in soil erosion whereas on the onset of monsoon, due to least vegetation activity, soil erosion could be drastically high.

4.2 Spectral Separability of LULC classes

Spectral response curves (Figure 7a-c) of three different seasons are being analysed in this section to assess how well aforementioned LULC classes are spectrally separable. Sequentially, for the month of January; cropland has least reflectance among all three LULC classes except in the fourth band i.e. near infrared where it is highest. Due to low reflectance of vegetation in most of the bands apart from NIR, it appears rather dark and thus giving lower reflectance. Noticeably, reflectance difference between cropland and badlands is the highest during January among all the seasons and bands combined altogether. For the month of April, reflectance difference between badlands and croplands is almost uniform in all bands. As all LULC classes are devoid of vegetation; bare soil is responsible for most of the reflectance. Lower reflectance from badlands can be attributed to shadow effects from constituting gullies. Lastly, for the month of October; reflectance of badlands is almost similar to cropland in the month of January except the difference between two classes is much lesser. The vegetation cover which covered whole cropland area during January is now covering the whole badland area. Despite this trend, there are still vegetation patches in the cropland which adulterate delineation of badlands from cropland (Figure 6c).

Levelled land and cropland have almost same trend of reflectance in all three seasons and also year-round (Figure 5 & Figure 7). Cultivation on levelled land (rolling topography) results in sparse vegetation therefore the reflectance is mixed i.e. partly from soil and partly from vegetation. Reflectance from soil makes levelled land brighter and thus put it above all other LULC classes in figure 7.

Since, the LU class of badlands has changed since 1971 as shown in Figures 8a & 8b; badlands were levelled to make them arable. It is expected that the vegetation activity of levelled land should increase over the years with so many years of cultivation. However, no significant trend was noticed in the vegetation activity in the past 12 years. This can be confirmed by the line graph (Figure 9) which does not show a straight increase in the NDVI values. Least activity is shown in the year 2002 (Figure 8 & 9),

which might be attributed to the fact of having less rain in that year. Inability to find a significant evolution of vegetation activity in levelled land might be due to the condition of soil is still poor i.e. high erosion, poor soil structure etc. and continuous levelling effort might not result in a better soil structure. Since only 12 years were considered; the reason might also due to the lack of longer time series.

4.3 Spectral Classification

Initially, four LULC classes were classified i.e. water body, badlands, cropland & levelled land. Accuracy assessment (Table 1) shows that levelled land has least accuracy (both producer's & user's). Low user's accuracy indicates high error due to commission i.e. other categories are falsely classified as levelled land. As also evident from Figure 5 & 7; levelled land has similar reflectance trend to cropland which explains low user's accuracy. This trend of low user's accuracy of levelled land is consistent in all three seasons. Mixing of reflectance also account for classification's low overall accuracy and low kappa value. An alternative approach is to merge cropland with levelled land and to classify image with two LULC classes i.e. badlands and other classes. With these two classes, areal extent of badlands can still be calculated easily. Furthermore, the accuracy of classification, with two LULC classes, has increased in all three seasons. January image performed better than the other two month's images (Table 2). User's and producer's accuracies show that the month of October was able to achieve best user's accuracy suggesting least error of commission but show low producer's accuracy indicating that error of elimination was high.

Kappa and overall accuracy, of the classification, for the month of January image outperformed the rest two. Therefore, bands from the January image were selected to further refine the classification with three different band selection methods (i.e. CV, TD and JM) (Table 3). One band is deleted at each step, classification and accuracy was carried out; some of the combinations were common to two methods. Overall accuracy show similar values indicating that almost all the combination gave equally correct classification. Kappa exhibited highest value to a combination with maximum number of bands. Difference in kappa values despite the similar overall accuracy is attributed to errors due to commission and omission. Figure 10 shows best classifications from all the three seasons: January, April and October.

However, levelled land is, indeed, a transitory class between badlands and cropland; it is not possible to estimate when badland would completely be turned into a flat cropland. Due to its rolling topography, it remains highly vulnerable to water erosion and thus the productivity is not as good as cropland's. Nonetheless, it is still profitable to cultivate levelled land especially with lentils and mustard as they have lesser water requirements. Levelled land contributes most to the dynamics of badlands but could not be spectrally separated successfully from cropland and badlands but estimating badlands accurately should be a measure towards estimating badlands dynamics.

Interestingly, the vegetation mapping band (NIR:band4) is always present in all the combinations which indicate the usefulness of NIR spectrum in mapping erosional features; this was also shown by Vrieling et al., (2007). Band selection methods i.e. CV, TD and JM delete bands with least variation and high correlation and thus the noise. This process leaves bands which contribute most to the classification and since NIR band is present in all the combinations, it proved very useful in the classification. Liberti et al (2009) used TM and ETM+ images to map badlands in the southern Italy where they have demonstrated that if slope and aspect is incorporated in the classification, accuracy to delineate badlands increases. This method was also used in this study but it did not return better accuracy; this can be attributed to two reasons 1) badlands in this study area are all observed in a wide (former) valley bottom whereas badlands in southern Italy are typically located on rather steep valley slopes in a mountainous environment and 2) lower resolution of DEM was used but higher resolution might improve the accuracy.

This method is primarily dependent on vegetation cover and thus can only be replicated to other areas where similar seasonal changes in vegetation are observed. Delays in the monsoon arrival can delay cropping seasons, therefore, it possible to expect some shift in the highest vegetation difference between cropland and badlands.

5 Conclusions

This study reports a special variation in vegetation activity in the lower Chambal valley, India. Initial separation of three LULC classes i.e. badlands, cropland and levelled land, resulted in noticeable differences in vegetation activities in three classes. Cropland and levelled land followed same annual trend of vegetation activity; this trend, actually,

represents two distinct cropping seasons in that area i.e. kharif (wet) season and rabi (dry) season. In contrast, vegetation activity in badlands is different from the rest two classes, on the onset of monsoon vegetation activity in badlands increases tremendously. Vegetation activity, then, slows down with the retreating monsoon and due to water scarcity and harsh climatic conditions; it reduces to minimum during summers. This contrast in vegetation activity separates badlands from cropland in the month of January when croplands are at the peak of cultivation and badlands have least vegetation activity and in the month of October when badlands are at the peak of vegetation activity due to monsoon and croplands has least due to beginning of rabi season. However, the NDVI values of levelled land follow those of cropland, but the former is much lower than the latter due to sparse cropping on its rolling topography.

Aforementioned contrast in vegetation was used to classify badlands by supervised classification. It was found that levelled land is a transitory land use class and has similar reflectance values to cropland. However, badlands were levelled for cultivation purposes; this study failed to find an expected increasing trend of vegetation activity in the levelled land. Levelled land, therefore, still has high soil erosion rates which hampers vegetation activity and spectral separability. It was found that the vegetation contrast between the badlands and croplands, which is highest in the month of January, is useful in segregating badlands from other LULC classes with supervised classification. The Landsat 5 band combination 1-5, 7 (VIS, NIR, SWIR) could be shown to yield the highest classification accuracy.

Acknowledgements

The first author would like to thank Erasmus Mundus External Program window 13 for financing author's stay at KU Leuven. The authors would also like to acknowledge the help of GeoEye foundation, who had provided the GeoEye image for this research.

References

Adams BP. 1987. Assessment of the 1987 Chambal Ravines Aerial Seeding Programme. Rome: FAO.

Alatorre LC, Beguería S, Vicente-Serrano S. 2011. Evolution of vegetation activity on vegetated, eroded, and erosion risk areas in the central Spanish Pyrenees, using multitemporal Landsat imagery. Earth Surface Processes and Landforms. 36:309–319.

Alatorre LC, Beguería S. 2009. Identification of eroded areas using remote sensing in a badlands landscape on marls in the central Spanish Pyrenees. CATENA. 76:182–190.

Beguería S. 2006a. Identifying erosion areas at basin scale using remote sensing data and GIS: a case study in a geologically complex mountain basin in the Spanish Pyrenees. International Journal of Remote Sensing. 27:4585–4598.

Beguería S. 2006b. Identifying erosion areas at basin scale using remote sensing data and GIS: a case study in a geologically complex mountain basin in the Spanish Pyrenees. International Journal of Remote Sensing. 27:4585–4598.

Borselli L, Torri D, Øygarden L, De Alba S, Martínez-Casasnovas JA, Bazzoffi P, Jakab G. 2006. Land Levelling. In: Boardman J, Poesen J, editors. Soil Erosion in Europe [Internet]. [place unknown]: John Wiley & Sons, Ltd; [cited 2012 Aug 13]; p. 643–658. Available from: http://onlinelibrary.wiley.com/doi/10.1002/0470859202.ch46/summary

Byrnes BH, Bumb BL. 1998. Population Growth, Food Production and Nutrient Requirements. Journal of Crop Production. 1:1–27.

Chander G, Markham BL, Helder DL. 2009. Summary of current radiometric calibration coefficients for Landsat MSS, TM, ETM+, and EO-1 ALI sensors. Remote Sensing of Environment. 113:893–903.

Chatterjee RS, Saha SK, Suresh Kumar, Sharika Mathew, Lakhera RC, Dadhwal VK. 2009. Interferometric SAR for characterization of ravines as a function of their density, depth, and surface cover. ISPRS Journal of Photogrammetry and Remote Sensing. 64:472–481.

Ciccacci S, Galiano M, Roma MA, Salvatore MC. 2009. Morphodynamics and morphological changes of the last 50 years in a badland sample area of Southern Tuscany (Italy). Zeitschrift für Geomorphologie. 53:273–297.

Dwivedi RS, Ramana KV. 2003. The delineation of reclamative groups of ravines in the Indo-Gangetic alluvial plains using IRS-1D LISS-III data. International Journal of Remote Sensing. 24:4347–4355.

Foody GM. 2002. Status of land cover classification accuracy assessment. Remote Sensing of Environment. 80:185–201.

Gallart F, Marignani M, Pérez-Gallego N, Santi E, Maccherini S. 2013. Thirty years of studies on badlands, from physical to vegetational approaches. A succinct review. CATENA. 106:4–11.

Geo Eye. 2009. Geo Eye Product Guide v1.0.1. 4 [Internet]. Available from: www.genesiis.com/pdf/2009_geoeye_product_guide.pdf

Gilland B. 2002. World population and food supply: can food production keep pace with population growth in the next half-century? Food Policy. 27:47–63.

Goslee SC. 2011. Analyzing Remote Sensing Data in R: The landsat Package. Journal of Statistical Software. 43:1–25.

Habib I. 1963. The agrarian system of Mughal India, 1556-1707. [place unknown]: Asia Publishing, London.

Huete A, Didan K, Miura T, Rodriguez E., Gao X, Ferreira L. 2002. Overview of the radiometric and biophysical performance of the MODIS vegetation indices. Remote Sensing of Environment. 83:195–213.

Kottek M, Grieser J, Beck C, Rudolf B, Rubel F. 2006. World Map of the Köppen-Geiger climate classification updated. Meteorologische Zeitschrift. 15:259–263.

Liberti M, Simoniello T, Carone MT, Coppola R, D'Emilio M, Macchiato M. 2009. Mapping badland areas using LANDSAT TM/ETM satellite imagery and morphological data. Geomorphology. 106:333–343.

Lillesand T, Kiefer RW. 1987. Remote Sensing and Image Interpretation. 2nd ed. [place unknown]: Wiley.

Marzolff I, Ries JB, Poesen J. 2011. Short-term versus medium-term monitoring for detecting gully-erosion variability in a Mediterranean environment. Earth Surface Processes and Landforms. 36:1604–1623.

McDonald RA. 1995. Corona: success for space reconnaissance, a look into the Cold War, and a revolution in intelligence. Photgrammetric Engineering & Remote Sensing. 61:689–720.

Metternicht GI, Zinck JA. 1998. Evaluating the information content of JERS-1 SAR and Landsat TM data for discrimination of soil erosion features. ISPRS Journal of Photogrammetry and Remote Sensing. 53:143–153.

Nachtergaele J, Poesen, J. 1999. Assessment of soil losses by ephemeral gully erosion using high-altitude (stereo) aerial photographs. Earth Surface Processes and Landforms. 24:693–706.

Nadal-Romero E, Vicente-Serrano SM, Jiménez I. 2012. Assessment of badland dynamics using multi-temporal Landsat imagery: An example from the Spanish Pre-Pyrenees. CATENA. 96:1–11.

National Remote Sensing Centre, India. 2011. Wastelands Atlas of India (Change Analysis Based on Multi-Temporal Satellite Data of 2005-06 and 2008-09) [Internet]. Available from: http://www.dolr.nic.in/WastelandsAtlas2011/Wastelands_Atlas_2011.pdf

Oostwoud Wijdenes DJ, Poesen J, Vandekerckhove L, Ghesquiere M. 2000. Spatial distribution of gully head activity and sediment supply along an ephemeral channel in a Mediterranean environment. CATENA. 39:147–167.

Pani P, Mohapatra SN. 2001. Delineation and monitoring of gullied and ravinous lands in a part of lower Chambal valley, India using remote sensing and GIS. In: Proc ACRS. Singapore.

Phillips C. 1998. The badlands of Italy: a vanishing landscape? Applied Geography. 18:243–257.

Plourde L, Congalton RG. 2003. Sampling Method and Sample Placement: How Do They Affect the Accuracy of Remotely Sensed Maps? Photogrammetric Engineering & Remote Sensing. 69:289–297.

Poesen JW., Hooke JM. 1997. Erosion, Flooding and Channel Management in Mediterranean Environments of Southern Europe. Progress in Physical Geography. 21:157–199.

R Development Core Team. 2011. R: A language and environment for statistical computing. R Foundation for Statistical Computing, Vienna, Austria [Internet]. [place unknown]. Available from: URL http://www.R-project.org/

Ranga V. 2013. GIS Based Gully Erosion Mapping & Modeling Using Multi-Spectral Spatial And Non-Spatial Data In Parts Of Ambah And Morena Tehsils Of Morena District, Madhya Pradesh. [PhD]. Gwalior, India: Jiwaji University.

Seginer I. 1966. Gully development and sediment yield. Journal of Hydrology. 4:236–253.

Sharma HS. 1979. The Physiography of the Lower Chambal Valley and Its Agricultural Development: A Study in Applied Geomorphology. [place unknown]: Concept Publishing Co.

Sharma HS. 1980. Ravine erosion in India [Internet]. [place unknown]: Concept Pub. Co. Available from: http://books.google.be/books?id=EJM1AAAAMAAJ

Silleos NG, Alexandridis TK, Gitas IZ, Perakis K. 2006. Vegetation Indices: Advances Made in Biomass Estimation and Vegetation Monitoring in the Last 30 Years. Geocarto International. 21:21–28.

Singh AN. 1984. Delineating Ravinous Areas on Aerial and Satellite Imagery-A comparative Study. Journal of the Indian Society of Remote Sensing. 12:49–54.

Singh B. 1977. Interpretation of satellite imagery for delineation of ravines. Journal of the Indian Society of Remote Sensing. 5:31–34.

Singh S, Agnihotri SP. 1987. Rill and Gully Erosion in the Subhumid Tropical Riverine Environment of Teonthar Tahsil, Madhya Pradesh, India. Geografiska Annaler Series A, Physical Geography. 69:227–236.

Sneddon J, Williams B, Savage J, Newman C. 1988. Erosion of a gully in duplex soils - Results of a long term photogrammetric monitoring program. Soil Res. 26:401–408.

Sohn H-G, Kim G-H, Yom J-H. 2004. Mathematical modelling of historical reconnaissance CORONA KH-4B Imagery. The Photogrammetric Record. 19:51–66.

Sujatha G, Dwivedi RS, Sreenivas K, Venkataratnam L. 2000. Mapping and monitoring of degraded lands in part of Jaunpur district of Uttar Pradesh using temporal spaceborne multispectral data. International Journal of Remote Sensing. 21:519–531.

Torri D, Calzolari C, Rodolfi G. 2000. Badlands in changing environments: an introduction. CATENA. 40:119–125.

Vandekerckhove L, Poesen J, Oostwoud Wijdenes D, Gyssels G. 2001. Short-term bank gully retreat rates in Mediterranean environments. CATENA. 44:133–161.

Vrieling A, de Jong SM, Sterk G, Rodrigues SC. 2008. Timing of erosion and satellite data: A multi-resolution approach to soil erosion risk mapping. International Journal of Applied Earth Observation and Geoinformation. 10:267–281.

Vrieling A, Rodrigues SC, Bartholomeus H, Sterk G. 2007. Automatic identification of erosion gullies with ASTER imagery in the Brazilian Cerrados. International Journal of Remote Sensing. 28:2723–2738.

Zinck JA, López J, Metternicht GI, Shrestha DP, Vázquez-Selem L. 2001. Mapping and modelling mass movements and gullies in mountainous areas using remote sensing and GIS techniques. International Journal of Applied Earth Observation and Geoinformation. 3:43–53.

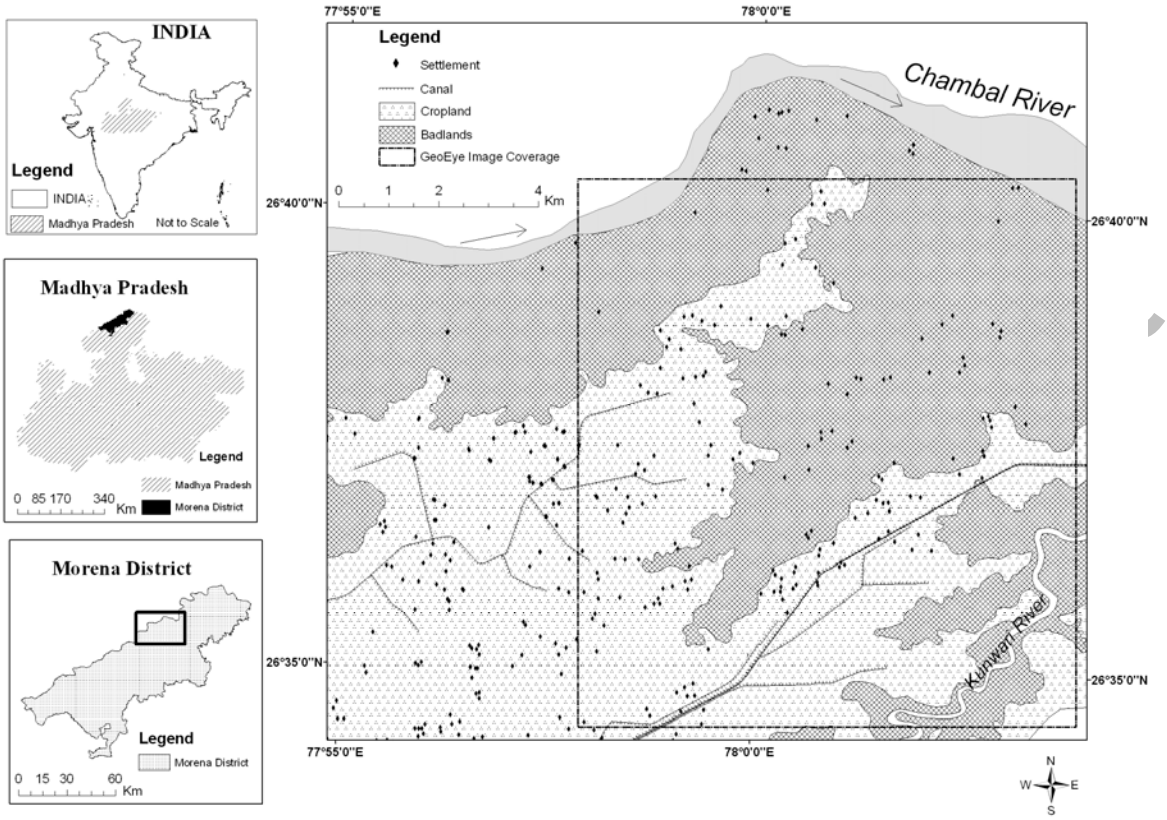

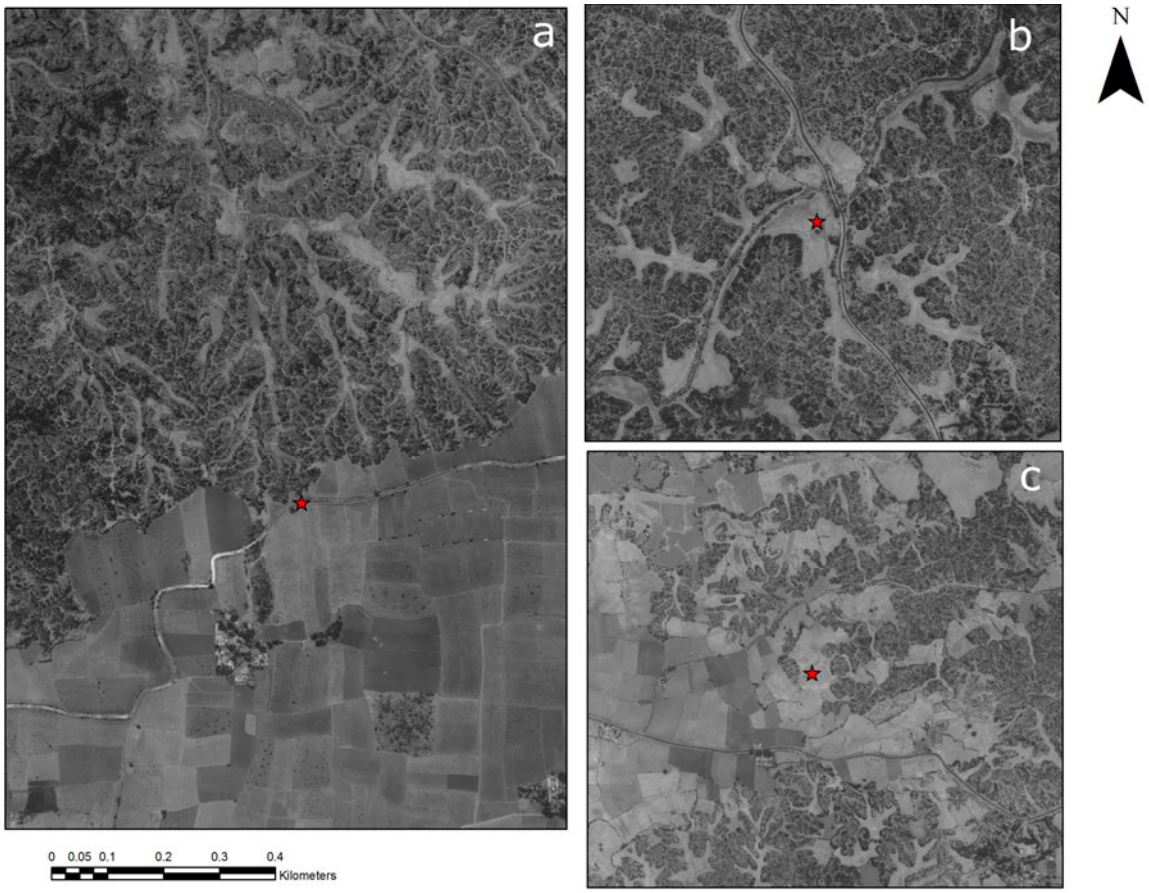

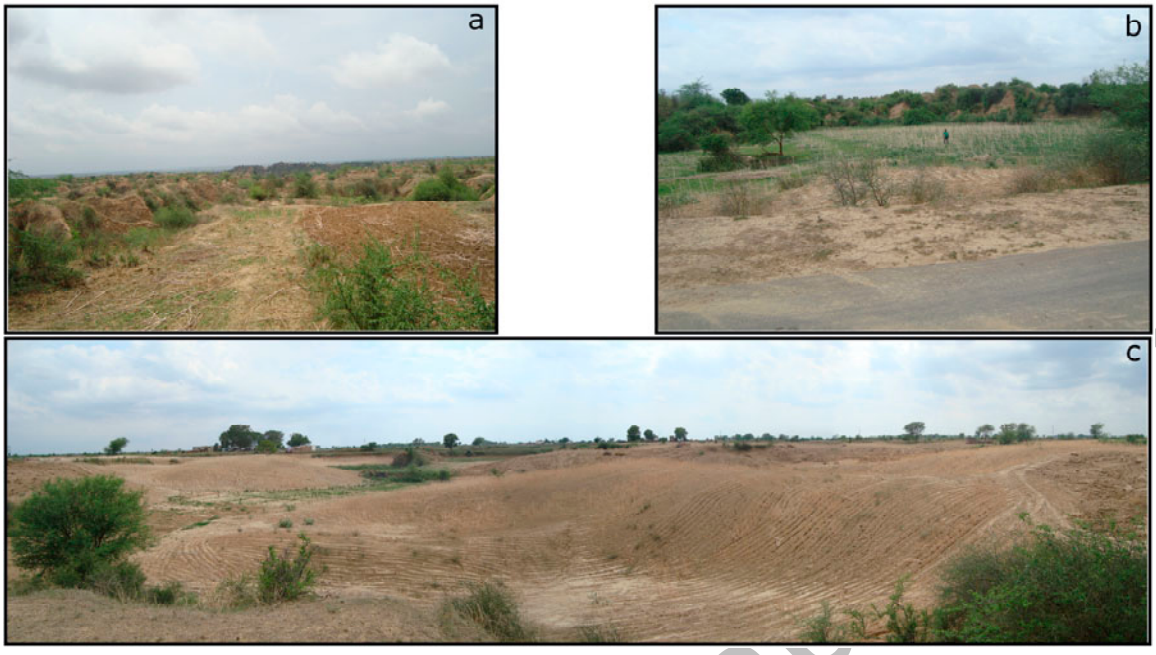

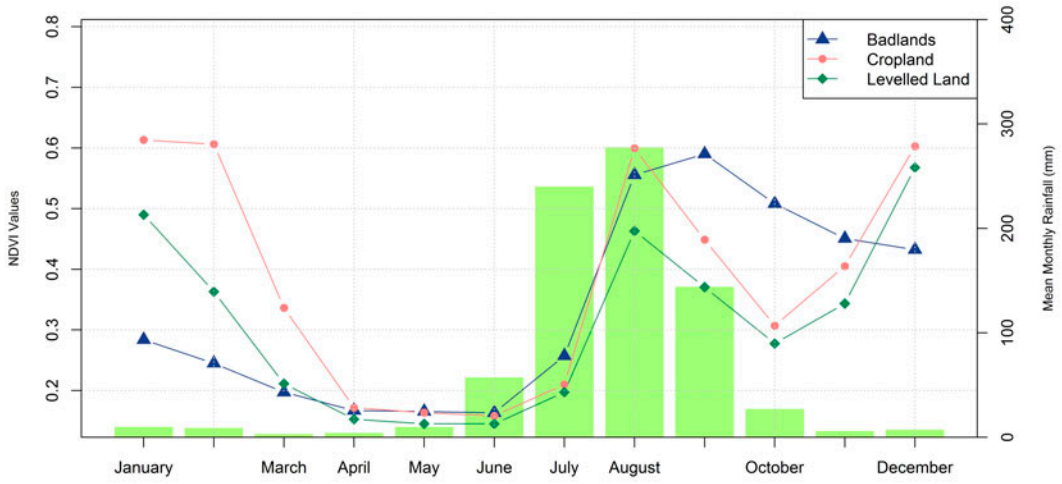

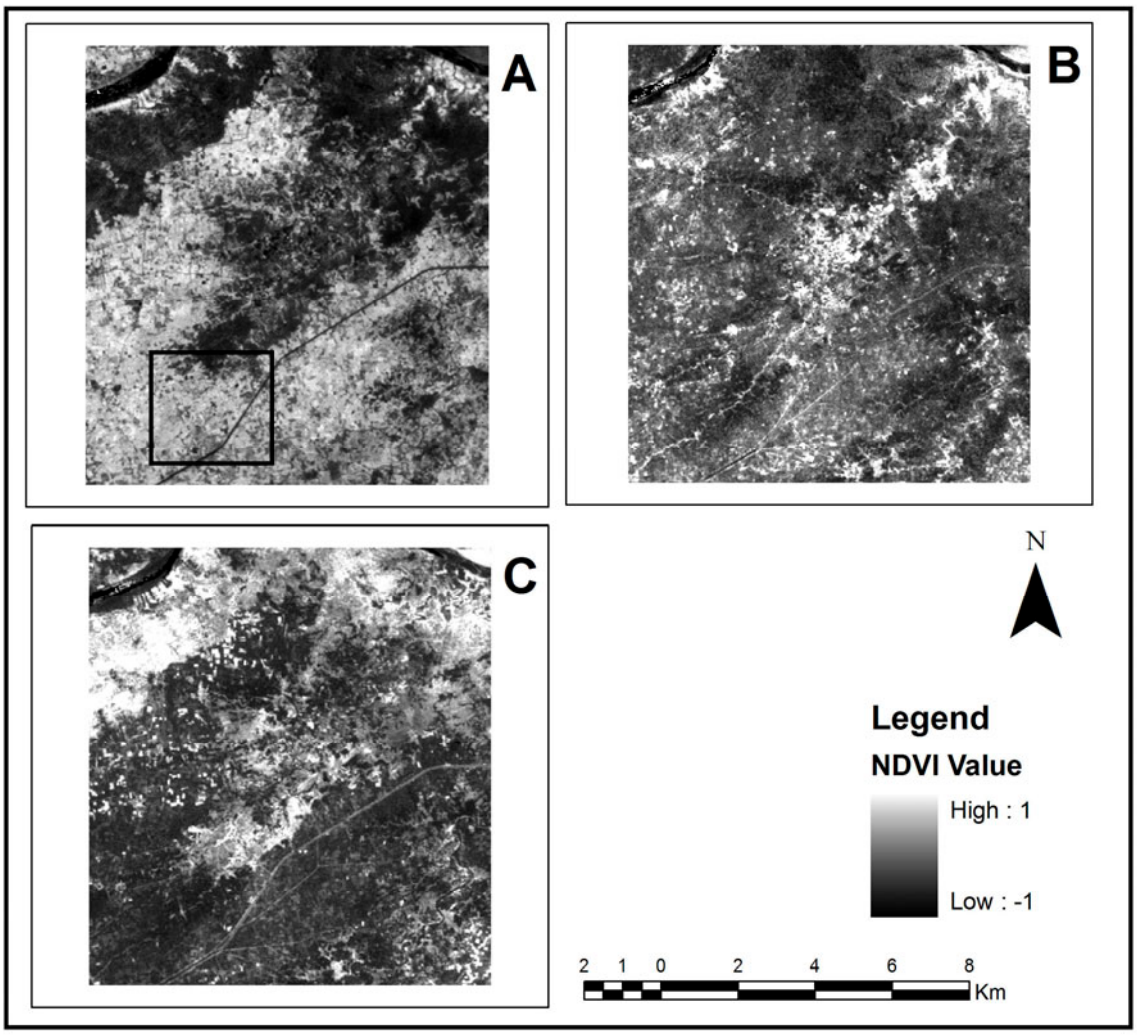

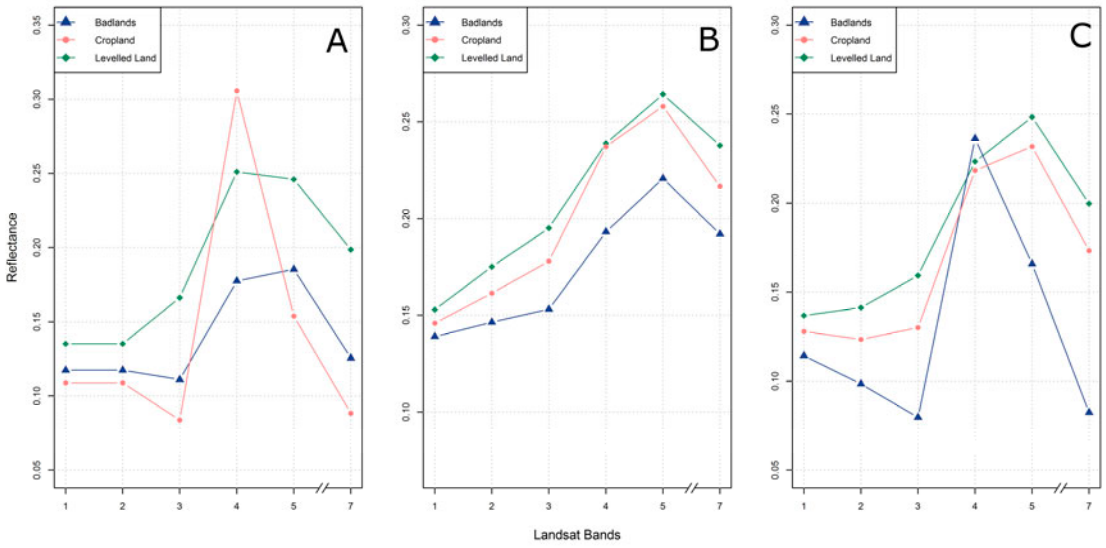

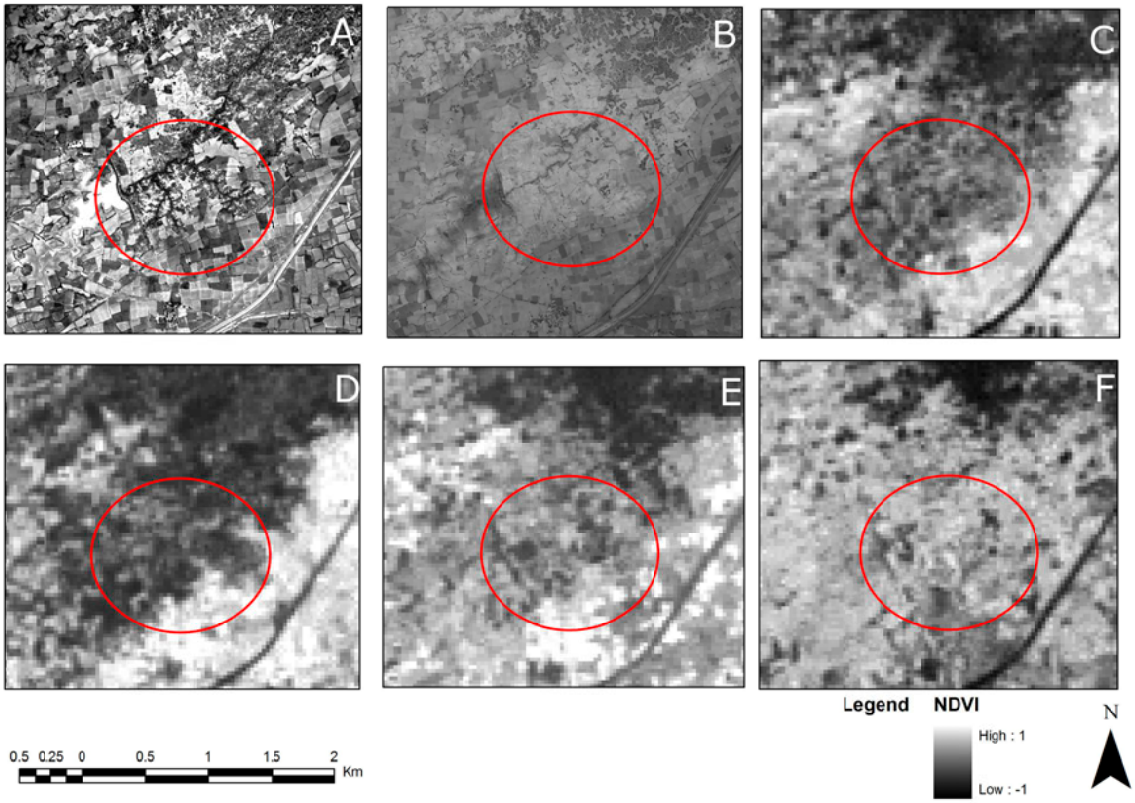

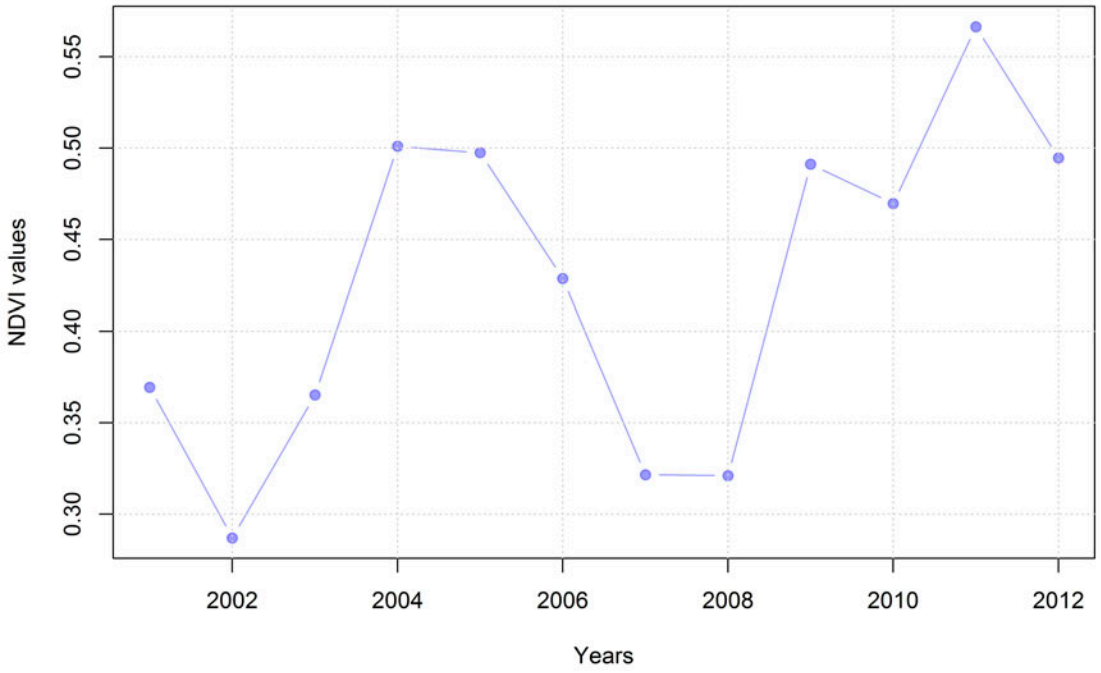

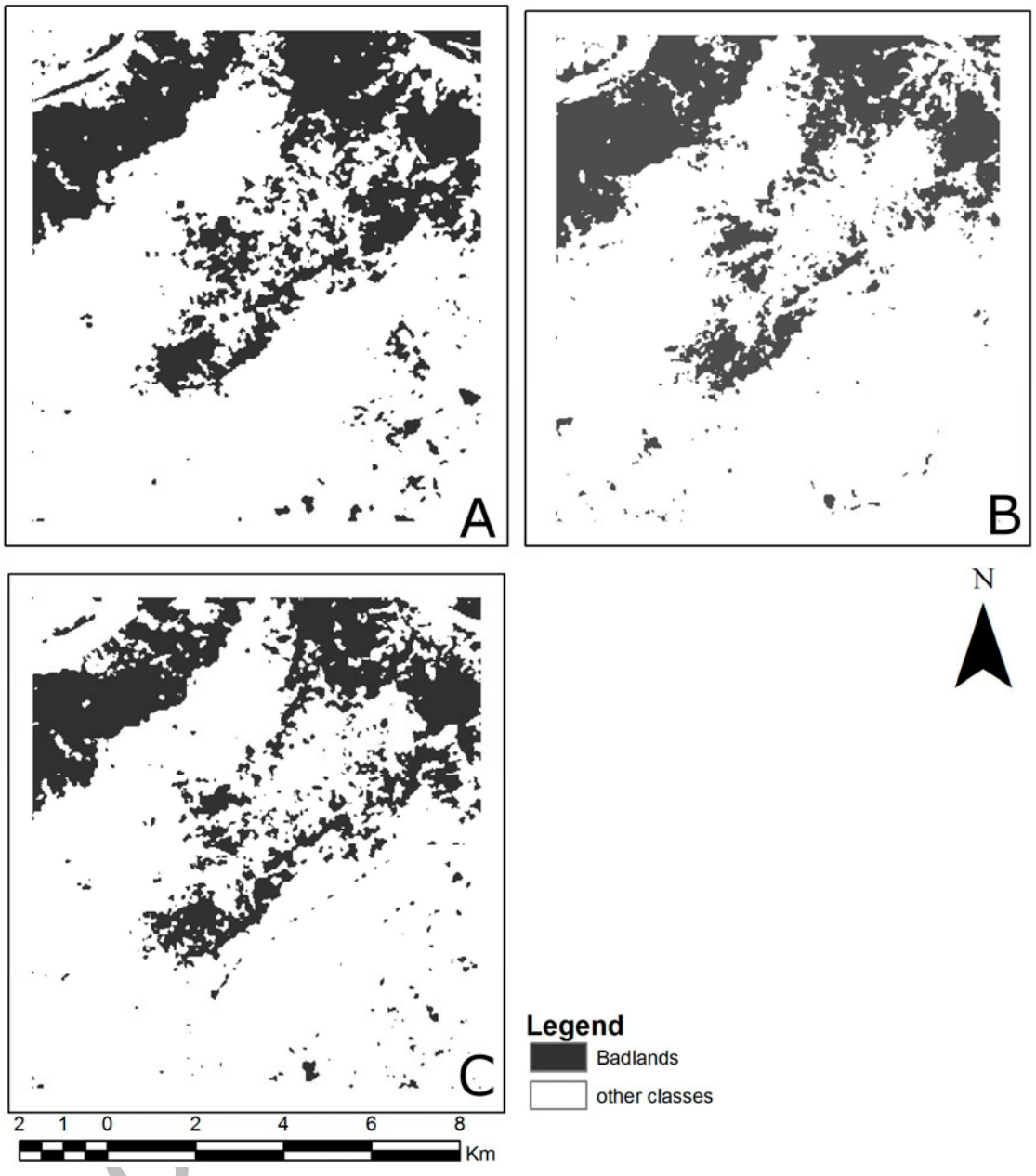

Table 1. Accuracies of three classified TM images from three different months i.e. January, April and October.

Month (image acquisition date)	LULC classes	Producer's Accuracy	User's Accuracy	Overall Accuracy (%)	Kappa
January (16-01-2011)	Water Body	100	41.1	71.81	0.57
	Badlands	71.7	92.3		
	Cropland	68.1	83		
	Levelled Land	79.2	36.1		
April (03-04-2010)	Water Body	100	46.6	71.03	0.53
	Badlands	80.2	77.7		
	Cropland	63.2	86.2		
	Levelled Land	61.9	41.1		
October (28-10-2010)	Water Body	100	53.8	69.7	0.51
	Badlands	79.2	77.2		
	Cropland	60	80		
	Levelled Land	63.6	42.2		

Table 2. Accuracies of three classified Landsat 5 TM images with their respective accuracies.

Month (image acquisition date)	LULC classes	User's Accuracy	Producer's Accuracy	Overall Accuracy	Kappa
January (16-01-2011)	Badlands	88.07	70.94	86.66	0.6906
	Other classes	86.12	94.94		
April (03-04-2010)	Badlands	90.35	57.64	83.26	0.5949
	Other classes	81.26	96.76		
October	Badlands	91.67	59.61	84.20	0.6188

(28-10-2010)	Other classes	82.04	97.15		

Table 3. Selected Landsat 5 TM bands from various methods and their respective accuracies. CV = Covariance-variation; TD = Transformed Divergence; JM = Jafferies Matusita.

Serial No.	Selected Bands	Method	Kappa	Overall Accuracy
1.	1-5,7	-	0.7026	86.66
2.	1-4,7	CV	0.6888	86.58
3.	1-5	TD	0.6931	86.66
4.	2-5,7	JM	0.6921	86.66
5.	2-4,7	CV	0.6913	86.66
6.	1,2,4,5	TD	0.6798	86.24
7.	2-5	JM	0.6903	86.58
8.	3,4,7	CV	0.6917	86.66
9.	2,4,5	TD, JM	0.6837	86.41